

Photochemistry

Photogeneration and Visualization of a Surface-Stabilized Dinitrene

Federico Frezza, Ana Sánchez-Grande, Sofia Canola,* Christophe Nacci, Jiří Klívar, Pingo Mutombo, Qifan Chen, José María Gómez-Fernandez, Carlos Sánchez-Sánchez, Jan Berger, Karl-Heinz Ernst, Irena G. Stará, José Ángel Martín-Gago,* Ivo Starý,* Leonhard Grill,* and Pavel Jelínek*

Abstract: Nitrenes are known as key intermediates in various chemical reactions. Nitrene transfer reactions are particularly effective for synthesizing nitrogen-containing compounds, where metal catalysts play a crucial role in controlling nitrene reactivity and selectivity. In this study, we demonstrate the formation of a stable surface-supported dinitrene on Au(111) through UV irradiation of its diazide precursor, characterized by scanning probe techniques. The photoreaction mechanism is elucidated with wavelength-dependent experiments and time-dependent density functional theory calculations. Our findings present the first real-space visualization of a metal nitrene adsorbed on a surface, highlighting its potential in catalysis and surface functionalization.

Nitrenes are highly reactive and short-lived species, playing an important role as intermediates for a plethora of chemical reactions.^[1,2] In the last few years, there was a booming interest in skeletal editing methods, where nitrenes are often involved in N-insertion processes.^[3–5] Furthermore, the use of nitrene transfer reactions involving metal-nitrenoid intermediates represents an efficient strategy for the synthesis of N-containing compounds.^[6] In such reactions, the first step is

the formation of a transition metal (TM) nitrene complex (see Scheme 1), which can further react towards the formation of new C–N bonds, e.g. through aziridination or C–H insertion. Several TMs including coinage metals have been reported to efficiently tame the nitrene reactivity, influencing its chemo- and enantioselectivity and catalyzing the reactions.^[7,8] In this regard, the stabilization of metal-nitrene complexes allows to follow the stepwise process, study the structure of the intermediate and understand the mechanisms of nitrene transfer reactions. Nowadays nitrenes are routinely obtained from azides via photochemical, thermal, or metal-mediated routes, with the elimination of dinitrogen as a side product.^[9–11] The photochemistry of azides has been thoroughly investigated:^[12–16] namely, singlet arylnitrenes can go through either a rearrangement or intersystem crossing, in the latter case leading to a triplet nitrene that can dimerize forming diazo compounds.^[17] Recently, a crystalline nitrene was synthesized by azide photolysis, presenting extraordinary stability.^[18]

Within this framework, a known successful method to study reactive compounds such as azides (and the respective intermediates like nitrenes) is on-surface chemistry under ultra-high vacuum (UHV) conditions by means of scanning probe microscopy at cryogenic temperatures, as widely demonstrated for open-shell carbon-based nanostructures.^[19] Organic azides on surfaces have been mainly studied as

[*] F. Frezza, Dr. A. Sánchez-Grande, Dr. S. Canola, Dr. P. Mutombo, Q. Chen, Dr. J. Berger, Prof. K.-H. Ernst, Prof. P. Jelínek
 Institute of Physics
 Czech Academy of Sciences
 Cukrovarnická 10, 16200, Prague 6, Czech Republic
 E-mail: canola@fzu.cz
 jelinek@fzu.cz

F. Frezza
 Faculty of Nuclear Sciences and Physical Engineering
 Czech Technical University in Prague
 Břehová 78/7, 11519 Prague 1, Czech Republic

Dr. C. Nacci, Prof. L. Grill
 Department of Physical Chemistry
 University of Graz
 Heinrichstraße 28, 8010 Graz, Austria
 E-mail: leonhard.grill@uni-graz.at

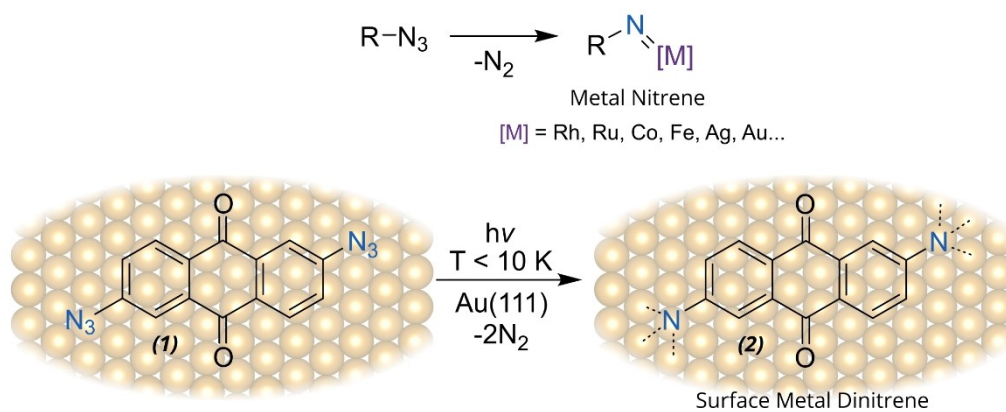
Dr. J. Klívar, Dr. I. G. Stará, Dr. I. Starý
 Institute of Organic Chemistry and Biochemistry
 Czech Academy of Sciences
 Flemingovo nám. 2, 16610 Prague 6, Czech Republic
 E-mail: ivo.starý@uochb.cas.cz

J. M. Gómez-Fernandez, Dr. C. Sánchez-Sánchez,
 Prof. J. Á. Martín-Gago
 Instituto de Ciencia de Materiales de Madrid,
 CSIC
 Cantoblanco, 28049 Madrid, Spain
 E-mail: gago@icmm.csic.es

Dr. J. Berger, Prof. P. Jelínek
 Regional Centre of Advanced Technologies and Materials
 Czech Advanced Technology and Research Institute (CATRIN)
 Palacký University
 78371 Olomouc, Czech Republic.

Prof. K.-H. Ernst
 Empa
 Swiss Federal Laboratories for Materials Science and Technology
 Überlandstrasse 129, 8600 Dübendorf, Switzerland

© 2025 The Author(s). Angewandte Chemie International Edition published by Wiley-VCH GmbH. This is an open access article under the terms of the Creative Commons Attribution License, which permits use, distribution and reproduction in any medium, provided the original work is properly cited.



Scheme 1. Top panel: nitrogen extrusion from azides leading to metal nitrene intermediates in solution chemistry. Bottom panel: in this paper we study the 2,6-diazaanthraquinone-9,10-dione precursor **1** and respective photogenerated dinitrene **2** stabilized on the Au(111) surface.

precursors of the azide-alkyne Huisgen cycloaddition reaction.^[20–22] In the context of on-surface chemistry, the use of light or tip manipulation as a stimulus offers a higher control compared to thermal-assisted reactions, opening the possibility for low-temperature reactions and thus facilitating the stabilization and study of reactive intermediates.^[23–25] While the role of carbene ligands in surface chemistry has been explored in the last years,^[26] and surface metal carbenes have been studied at the nanoscale by scanning probe techniques,^[23,27–29] this characterization is still lacking for nitrenes due to their elusive nature.^[30–32]

Here, we report a comprehensive scanning tunneling microscopy (STM), non-contact atomic force microscopy (ncAFM), and computational study of a diazido anthraquinone molecule **1** and its photochemical activity on a Au(111) substrate, leading to the formation of a stable surface-supported dinitrene **2** (see Scheme 1). To this aim, we sublimed **1** on a Au(111) surface under UHV conditions, revealing the growth of large islands. Subsequently, upon UV irradiation, we observe the selective transformation into a dinitrene anthraquinone **2** stabilized by the underlying Au(111). Ultimately, to rationalize the mechanism triggering the photoactivation of **1** and the role of the metal substrate, we performed wavelength-dependence experiments, supported by time-dependent density functional theory calculations (TD-DFT). Altogether, we report the real-space visualization of a metal nitrene adsorbed on a surface through a light induced reaction of azide functional groups, with prospects in the catalytic synthesis of N-containing compounds or surface functionalization through strongly interacting molecular compounds.

Compound **1** was synthesized following the route described in Scheme S1.^[33] It was designed to expect flat adsorption on the surface, allowing SPM characterization, and its symmetry should lead to unambiguous adsorption mode. Furthermore, it proved to be stable enough to survive all the purification steps and thermal sublimation in UHV. After the solution synthesis, we studied the thermal stability of **1**: at 185 °C the molecules decompose, as visible in the supplementary video. The limited thermal stability of **1** calls for different reaction stimulus, and in this regard, photo-

chemistry offers a convenient option to carry out reactions at room temperature (RT) or even at cryogenic temperatures and on a large scale. Therefore, we recorded the UV/Vis absorption spectrum of **1** in dichloromethane (DCM) solution (Figure S1), which shows a first absorption band centered around 350 nm, followed by more intense bands at higher energies (ca. 310 nm and 275 nm). Next, the molecular precursor **1** was sublimed at 135 °C on a Au(111) crystal kept at RT. After sublimation, we observe large and homogeneous islands extended throughout the surface, as illustrated in Figure 1a. Precursor **1** self-assembles forming closed-packed islands, exhibiting unit cell parameters of $a = 8.2 \text{ \AA}$, $b = 12.8 \text{ \AA}$ and $\alpha = 75^\circ$ (see Figure 1b). Organic azides are typically very reactive and after sublimation onto

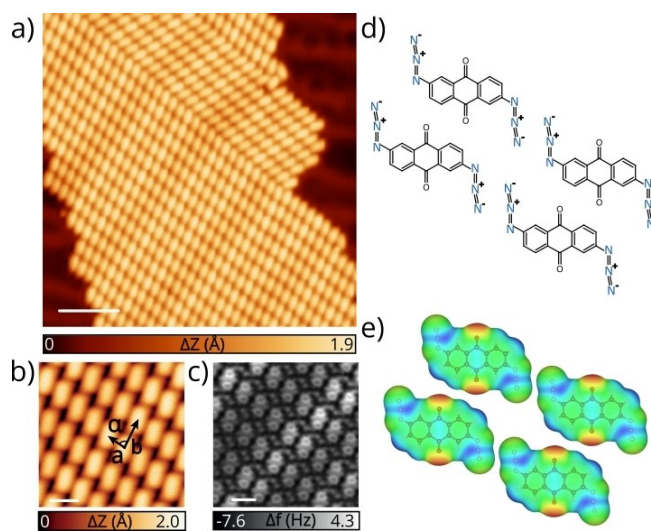


Figure 1. Structural characterization of diazide **1** on Au(111). a) Overview STM image of a closed-packed island of **1** on Au(111). ($V_b = 315 \text{ mV}$, $I_t = 50 \text{ pA}$ and scale bar = 5 nm). b) Zoom-in STM image showing the unit cell parameters. ($V_b = 50 \text{ mV}$, $I_t = 70 \text{ pA}$ and scale bar = 1 nm). c) NcAFM image of b). ($V_b = 1 \text{ mV}$, scale bar = 1 nm). d) Chemical sketch of the self-assembly of **1** on Au(111). e) Calculated electrostatic potential surface of **1** in gas phase showing the charge distributions and the proposed intermolecular interaction.

a coinage metal surface they immediately decompose.^[20,30] In order to confirm that **1** remains intact after deposition on Au(111), we performed ncAFM experiments. Figure 1c shows a high-resolution ncAFM image where, importantly, all molecules remain intact after sublimation at RT, in contrast to previous works on organic azides on surfaces.^[30] The azido groups from adjacent transversal molecules are observed as two bright protrusions in between the molecules, suggesting intermolecular interactions. One of the main resonance forms of azido groups contains one nitrogen atom positively charged followed by another one negatively charged, as exemplified in Figure 1d for **1**. We can assume that these charges are retained on the surface, as visible in the comparison of calculated electrostatic maps of **1** in gas phase and on the Au(111) surface (Figure S2). Thus, we rationalize the molecular self-assembly with an interplay between electrostatic interactions among azido groups and O...H hydrogen bonds (see electrostatic potential maps in Figure 1e).^[34] Due to the prochirality of **1**, we observe two chiral domains on the surface (see Figure S3), which can coexist on the same island. To investigate the molecule-substrate interaction, we conducted force-distance spectroscopic ($\Delta f(Z)$) measurements on different sites of the molecule and on Au(111) (see Figure S4) revealing an adsorption height of approximately 3 Å and confirming its planarity. This is in good agreement with the calculated DFT-optimized geometry of the single neutral molecule **1** on Au(111), showing a molecule-surface distance of 3.2 Å, compatible with a weak physisorption. Therefore, the electronic structure of **1** is only slightly perturbed by the

surface, as shown by the calculated projected density of states (PDOS) in Figure S4 for both the free-standing and adsorbed molecule.

Having confirmed that **1** adsorbs intact and planar on Au(111), we can investigate its photoreactivity, aiming at the generation of stabilized dinitrenes. We illuminated the sample at low temperature ($T < 10$ K) with monochromatic UV light ($\lambda = 266$ nm or 360 nm) targeting the excitation corresponding to the two absorption bands in the UV/Vis spectrum of **1** (Figure S1). In both cases we observe a clear change in the STM features after few minutes of illumination (see Figure S5), where each molecule is observed with the shape of three lobes, in contrast to diazide **1** which is essentially featureless. Figure 2a shows the same molecular island before and after 20 minutes of UV irradiation, imaged at the same bias voltage, where all molecules in the island show the same new features in the STM contrast. We investigated the chemical changes in **1** after illumination by ncAFM measurements. While the intact precursor lies flat and interacts weakly with the Au(111) (see simulated and experimental ncAFM in Figure 2b and calculated adsorption geometry in Figure 2c), the scenario changes after irradiation. As shown in Figure 2d, we cannot resolve the entire backbone of the molecule anymore in ncAFM, as only the central ring is visible. We assign this new product to dinitrene **2** (see Scheme 1), which is bent towards the Au(111) due to its high reactivity. The comparison between the simulated ncAFM image of **2** and the experiments (Figure 2d) validates our hypothesis, thus we can conclude that the illumination of **1** induces the release of two

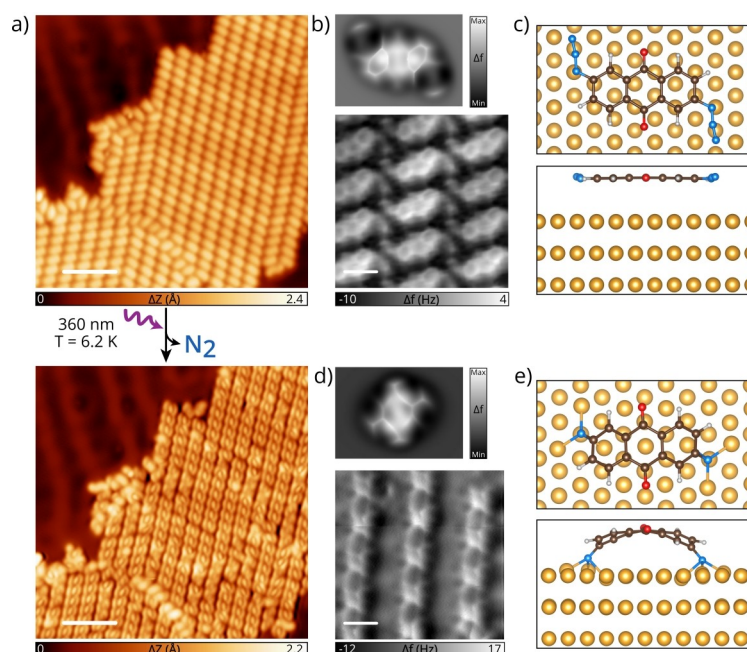


Figure 2. Light-induced generation of dinitrene **2** from azide **1**. a) Overview STM image of the same molecular island of **1** on Au(111) before and after illumination at 360 nm for 20 minutes ($V_b = 200$ mV, $I_t = 150$ pA and scale bar = 4.2 nm for both images). b) Simulated (top panel) and experimental (bottom panel) ncAFM image ($V_b = 2$ mV and scale bar = 7 Å) of **1** on Au(111). c) Top and side view of the calculated adsorption geometry of **1** on Au(111). d) Simulated (top panel) and experimental (bottom panel) ncAFM image of **2** on Au(111) ($V_b = 1$ mV and scale bar = 7 Å). e) Top and side view of the calculated adsorption geometry of **2** on Au(111).

molecular N₂ and the formation of the surface-supported dinitrene. The photogenerated product **2** shows a new conformation, suggesting a strong interaction with the surface inducing a nonplanar geometry, as corroborated in the DFT optimized geometry of **2** on Au(111) (Figure 2e). The calculations show an important interaction between the nitrene and the surface: the change in the adsorption geometry is accompanied by a charge redistribution, consisting in an accumulation of electron density around the N atoms, each one interacting with three underlying gold atoms, as shown in Figure S6. The strong interaction between the nitrene and the surface quenches its reactivity, similarly to carbenes on Ag(111),^[23] making it stable enough to be imaged. We highlight the high yield of the reaction and its selectivity: mainly product **2** is observed (we determined a yield of more than 90%), and very few molecules present an intermediate mononitrene.

The generation of the dinitrene species **2** can also be followed step-by-step by local tip manipulation. In this case, we observe first the formation of the intermediate mononitrene and subsequent formation of **2**. A detailed description of the process is depicted in Figure S7. Hence, we demonstrated the formation of a nitrene on a metal surface either locally by stepwise tip manipulation, or on larger areas via UV irradiation. After forming **2** at LT, we examined its reactivity upon thermal activation. Annealing at 240 °C post-illumination leads to the hydrogenation of the dinitrene, yielding diamino anthraquinone (**3**) along with other disordered structures (see Figure S8). Product **3** forms hydrogen-bonded 1D assemblies.

It is important to mention that thermal activation of **1** on Au(111) at 240 °C results in the formation of various compounds and disordered dendritic structures. As shown in Figure S9, we investigated the chemical structure of the products by STM and ncAFM, revealing a mixture of different compounds where the majority of the molecules have lost N₂. We performed quantum mechanics/molecular mechanics (QM/MM) calculations to rationalize the mechanism, which is mediated by single Au adatoms^[35,36] inducing the cleavage of the N=N bond, see Figure S10. Nevertheless, none of the products observed after annealing corresponds to the dinitrene anthraquinone **2**, while the light-induced reaction shows a high selectivity and yield toward the formation of **2** and opens a new reaction pathway to selectively form product **3** (Figure S8). Thus, the loss of molecular nitrogen towards the formation of a stable nitrene on a surface is not accessible by thermal activation.

To investigate the mechanistic aspects behind the processes involved in the photolytic N=N bond cleavage in **1** (red bond in the inset of Figure 3e), including the role of the metallic substrate, we probed the light response of **1** after illuminating at three selected wavelengths (266 nm, 360 nm and 450 nm) rationalizing the results with TD-DFT calculations, as summarized in Figure 3. The experimental and calculated absorption spectra in DCM solvent, together with a schematic representation of the vertical excited states, are displayed in Figure 3a,b. The three wavelengths employed in the experiments are also highlighted. Note that from the calculated absorption spectrum (Table S1), the first excited

state (S₁) is spectroscopically dark and is dominated by a $n\pi^*$ transition from an occupied orbital mainly localized on the carbonyl lone pairs (n_{CO}) to a virtual delocalized π orbital (see Figure S11). The intense absorption peaks correspond to higher excited states (respectively S₄, S₈ and S₉), dominated by transitions of $\pi\pi^*$ character, namely involving π orbitals delocalized on the whole conjugated system. We chose to illuminate 360 nm and 266 nm in order to match two different intense absorption bands in solution and 450 nm, which is below the molecular absorption threshold. Since all the experiments are carried out on a metallic surface, we must consider two possible excitation mechanisms: direct intramolecular excitation and hot electron attachment (HEA) from the metallic surface, where an excited photoelectron is attached to an unoccupied molecular orbital.^[37,38]

As shown above, illumination at 360 nm and 266 nm leads to the formation of the same product with a very high yield (>90%) after only a few minutes of illumination. When illuminating at 450 nm, no photoinduced processes should occur if we assume a negligible role from the substrate. However, we observe a partial photoconversion of **1** into **2**, with a yield around 26% (see Figure 3d and S12). Note that in order to reliably compare the results obtained at different wavelengths, we irradiated the sample at 360 nm and 450 nm with the same optical power, measured in a parallel setup (details in the methods) for 1 hour, the respective STM images after illumination are visible in Figure 3c,d (images before illumination for both samples are shown in Figure S13 as a comparison).

To rationalize the experimental results, we performed calculations showing the evolution of the excited states energies following the elongation of the N=N bond cleaved in the photoinduced process. As previously discussed, the excitation at 360 nm pumps the molecular system in the S₄ state (Figure 3b and 3e, red line at $d_{\text{NN}}^{\text{eq}}$, and Figure 3f red). At the molecular equilibrium geometry (at which the photoexcitation occurs), the state S₅ (Table S1, Figure 3e yellow line at $d_{\text{NN}}^{\text{eq}}$ and Figure 3f yellow) is nearby in energy (approx. 0.1 eV above S₄) and dominated by the $\pi\pi_{\text{az}}^*$ transition from a π occupied orbital to a virtual one localized on the azide fragments (π_{az}). Interestingly, upon minimal bond elongation (as low as 0.05 Å), the $\pi\pi_{\text{az}}^*$ state crosses below $\pi\pi^*$ (in energy) with almost no barrier and, due to its strong dissociative character along d_{NN} bond length coordinate (no minimum found), its energy drops until becoming the lowest excited state at only 0.3 Å of elongation (i.e. at $d_{\text{NN}} \sim 1.5$ Å). Hence, following photoexcitation promoting the system to the active S₄ $\pi\pi^*$ state (at $d_{\text{NN}}^{\text{eq}}$), a fast conversion to the dissociative $\pi\pi_{\text{az}}^*$ state can occur, leading to an efficient N=N dissociation. This is in line with the observed high yield and fast process of the present experiments (with $\lambda = 360$ nm) and with previous studies of the photophysical processes preceding azides photodissociation.^[39–43]

As another deactivation path after photoexcitation, the molecule can reach S₁ state via internal conversion (Kasha rule).^[44] Upon bond elongation (about 0.3 Å), S₁ acquires $\pi\pi_{\text{az}}^*$ dissociative character (Figure 3f yellow, Table S1),

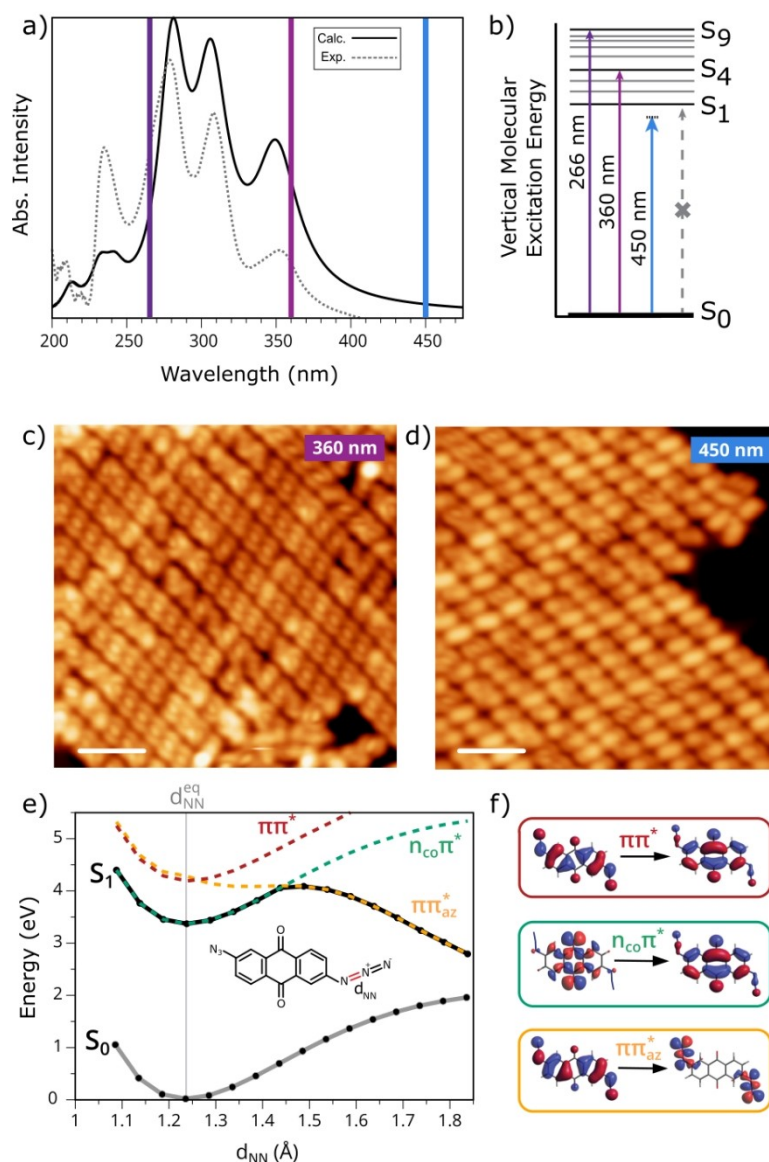


Figure 3. Insight into the light-induced reaction of **1**. a) Calculated (solid line, Lorentzian broadening, rigid shift of -0.55 eV) and experimental (dashed) absorption spectra of **1** in DCM solvent, where the three used wavelengths are highlighted. b) Scheme of vertical excited states c) STM image of a molecular island after illumination at 360 nm ($V_b = 100$ mV and $I_t = 100$ pA, scale bar = 3 nm). d) STM image of a molecular island after illumination at 450 nm ($V_b = 100$ mV and $I_t = 105$ pA, scale bar = 3 nm). e) Calculated potential energy curves upon elongation of the N=N bond (red in the inset): ground state S_0 (solid grey curve) and first excited state S_1 (solid black curve). The colored dashed curves follow the energy evolution of the excited state dominated by the transition indicated with the same color (the states at the equilibrium geometry d_{NN}^{eq} correspond to S_1 , S_4 , and S_5). f) Molecular orbitals involved in the relevant transitions. We can see how upon N=N elongation the transition from a π orbital to an orbital localized on the azido moiety (yellow) tends to lower its energy, giving S_1 a dissociative character at longer d_{NN} lengths.

suggesting that also in this case the dissociation can occur along the black curve in Figure 3e, provided the overcoming of an energetic barrier that lowers the overall efficiency of this process. In the case of excitation at 266 nm, similar experimental results suggest similar processes that evolve starting from the higher excited state S_9 .

Lastly, we can interpret the non-negligible yield after irradiation at 450 nm, that is below the energy necessary to promote the molecule to the first excited state via photoexcitation, with a contribution from the metallic substrate through HEA. Thus, this mechanism is also involved in the

process, although in a less efficient way, resulting in a lower photoconversion yield. A similar effect was observed in the photodecomposition of azides in the presence of a Pd catalyst, extending their photoreactivity to longer wavelengths.^[45]

We can deduce that the predominant process taking place is molecular photoexcitation, due to the low interaction between the molecule and the metallic substrate. However, the contribution from HEA mechanism is not negligible and thanks to the synergy between the two processes occurring in the light-mediated reaction, we

observe an efficient photochemical reaction on Au(111) that generates dinitrenes with high yield and selectivity.

We conclude that in the two proposed reaction mechanisms, the photochemical reaction is driven by the presence of the dissociative excited state localized on the azido moiety (yellow state in Figure 3f), leading to the N=N cleavage and the consequent nitrene formation and surface-mediated stabilization.

In summary, we report the generation and characterization of a dinitrene on a metal surface, synthesized by photolysis of its diazide precursor. While diazide is only physisorbed on Au(111), the photogenerated dinitrene interacts strongly with the substrate, that quenches its reactivity, allowing the characterization by scanning probe techniques. Our findings pave the way for understanding and tuning (di)nitrene reactivity on surfaces, offering new prospects in nitrene surface chemistry and surface functionalization. Furthermore, we performed wavelength-dependent experiments and TD-DFT calculation, rationalizing the molecular states involved in the photodissociation, highlighting a synergy between molecular photoexcitation and hot electron attachment.

Acknowledgements

A.S-G acknowledges the funding from the European Union and the Czech Ministry of Education, Youth and Sports (Project: MSCA Fellowship CZ FZU I-CZ.02.01.01/00/22_010/0002906). S.C. acknowledges the “Lumina Quaeruntur fellowship” of the Czech Academy of Sciences and computational resources from the project “e-Infrastruktura CZ” (e-INFRA CZ LM2018140) supported by the Ministry of Education, Youth and Sports of the Czech Republic. C.N. and L.G. thank the Austrian Science Foundation (FWF) for funding through projects P 33527-N and I 5145-N, respectively. P.J. acknowledges the financial support of Czech Science Foundation 21-17194L and the CzechNanoLab Research Infrastructure supported by MEYS CR (LM2023051). Open Access publishing facilitated by Fyzikální ústav Akademie věd České republiky, as part of the Wiley - CzechELib agreement.

Conflict of Interest

The authors declare no conflict of interest.

Data Availability Statement

The data that support the findings of this study are available from the corresponding author upon reasonable request.

Keywords: azide · metal surface · nitrene · photochemistry · scanning probe microscopy

- [1] P. F. Kuijpers, J. I. van der Vlugt, S. Schneider, B. de Bruin, *Chem. Eur. J.* **2017**, *23*, 13819–13829.
- [2] G. Dequirez, V. Pons, P. Dauban, *Angew. Chem. Int. Ed.* **2012**, *51*, 7384–7395.
- [3] M. Peplow, *Nature* **2023**, *618*, 21–24.
- [4] J. C. Reisenbauer, O. Green, A. Franchino, P. Finkelstein, B. Morandi, *Science* **2022**, *377*, 1104–1109.
- [5] S. C. Patel, N. Z. Burns, *J. Am. Chem. Soc.* **2022**, *144*, 17797–17802.
- [6] D. M. Sawant, G. Joshi, A. J. Ansari, *iScience* **2024**, *27*, 109311.
- [7] L.-W. Ye, X.-Q. Zhu, R. L. Sahani, Y. Xu, P.-C. Qian, R.-S. Liu, *Chem. Rev.* **2021**, *121*, 9039–9112.
- [8] W. Liu, I. Choi, E. E. Zerull, J. M. Schomaker, *ACS Catal.* **2022**, *12*, 5527–5539.
- [9] S. Bräse, C. Gil, K. Knepper, V. Zimmermann, *Angew. Chem. Int. Ed.* **2005**, *44*, 5188–5240.
- [10] K. Shin, H. Kim, S. Chang, *Acc. Chem. Res.* **2015**, *48*, 1040–1052.
- [11] M. Minozzi, D. Nanni, P. Spagnolo, *Chem. Eur. J.* **2009**, *15*, 7830–7840.
- [12] Elisa. Leyva, M. S. Platz, Gabriele. Persy, Jakob. Wirz, *J. Am. Chem. Soc.* **1986**, *108*, 3783–3790.
- [13] J. Soto, J. C. Otero, *J. Phys. Chem. A* **2019**, *123*, 9053–9060.
- [14] N. Gritsan, M. Platz, in *Organic Azides*, John Wiley & Sons, Ltd, **2009**, pp. 311–372.
- [15] A. K. Schrock, G. B. Schuster, *J. Am. Chem. Soc.* **1984**, *106*, 5234–5240.
- [16] G. B. Schuster, M. S. Platz, in *Advances in Photochemistry* (Eds.: D. H. Volman, G. S. Hammond, D. C. Neckers), John Wiley & Sons, Inc., Hoboken, NJ, USA, **2007**, pp. 69–143.
- [17] E. Leyva, M. S. Platz, E. Moctezuma, *J. Photochem. Photobiol.* **2022**, *11*, 100126.
- [18] M. Janssen, T. Frederichs, M. Olaru, E. Lork, E. Hupf, J. Beckmann, *Science* **2024**, *385*, 318–321.
- [19] D. G. de Oteyza, T. Frederiksen, *J. Phys. Condens. Matter* **2022**, *34*, 443001.
- [20] F. Bebensee, C. Bombis, S.-R. Vadapoo, J. R. Cramer, F. Besenbacher, K. V. Gothelf, T. R. Linderoth, *J. Am. Chem. Soc.* **2013**, *135*, 2136–2139.
- [21] O. Díaz Arado, H. Mönig, H. Wagner, J.-H. Franke, G. Langewisch, P. A. Held, A. Studer, H. Fuchs, *ACS Nano* **2013**, *7*, 8509–8515.
- [22] S. Stolz, M. Bauer, C. A. Pignedoli, N. Krane, M. Bommert, E. Turco, N. Bassi, A. Kinikar, N. Merino-Diez, R. Hany, H. Brune, O. Gröning, R. Widmer, *Commun. Chem.* **2021**, *4*, 1–7.
- [23] J. Mieres-Perez, K. Lucht, I. Trosien, W. Sander, E. Sanchez-Garcia, K. Morgenstern, *J. Am. Chem. Soc.* **2021**, *143*, 4653–4660.
- [24] F. Albrecht, S. Fatayer, I. Pozo, I. Tavernelli, J. Repp, D. Peña, L. Gross, *Science* **2022**, *377*, 298–301.
- [25] F. Frezza, A. Sánchez-Grande, S. Canola, A. Lamancová, P. Mutombo, Q. Chen, C. Wäckerlin, K.-H. Ernst, M. Muntwiler, N. Zema, M. Di Giovannantonio, D. Nachtigallová, P. Jelínek, *Angew. Chem. Int. Ed.* **2024**, *63*, e202405983.
- [26] A. V. Zhukhovitskiy, M. J. MacLeod, J. A. Johnson, *Chem. Rev.* **2015**, *115*, 11503–11532.
- [27] L. Jiang, B. Zhang, G. Médard, A. P. Seitsonen, F. Haag, F. Allegretti, J. Reichert, B. Kuster, J. V. Barth, A. C. Papageorgiou, *Chem. Sci.* **2017**, *8*, 8301–8308.
- [28] A. Bakker, A. Timmer, E. Kolodzeiski, M. Freitag, H. Y. Gao, H. Mönig, S. Amirjalayer, F. Glorius, H. Fuchs, *J. Am. Chem. Soc.* **2018**, *140*, 11889–11892.
- [29] A. Bakker, M. Freitag, E. Kolodzeiski, P. Bellotti, A. Timmer, J. Ren, B. Schulze Lammers, D. Mook, H. W. Roesky, H. Mönig, S. Amirjalayer, H. Fuchs, F. Glorius, *Angew. Chem. Int. Ed.* **2020**, *59*, 13643–13646.

- [30] J. Hellerstedt, A. Cahlik, O. Stetsovych, M. Švec, T. K. Shimizu, P. Mutombo, J. Klívar, I. G. Stará, P. Jelínek, I. Starý, *Angew. Chem. Int. Ed.* **2019**, *58*, 2266–2271.
- [31] M. Willenbockel, R. J. Maurer, C. Bronner, M. Schulze, B. Stadtmüller, S. Soubatch, P. Tegeder, K. Reuter, F. S. Tautz, *Chem. Commun.* **2015**, *51*, 15324–15327.
- [32] K. T. Wong, J. T. Tanskanen, S. F. Bent, *Langmuir* **2013**, *29*, 15842–15850.
- [33] B.-C. Liao, B.-H. Jian, M.-J. Wu, J.-T. Lee, *ACS Appl. Energ. Mater.* **2023**, *6*, 8581–8589.
- [34] J. Y. Kim, W. J. Jang, H. Kim, J. K. Yoon, J. Park, S.-J. Kahng, J. Lee, S. Han, *Appl. Surf. Sci.* **2013**, *268*, 432–435.
- [35] J. I. Mendieta-Moreno, B. Mallada, B. de la Torre, T. Cadart, M. Kitora, P. Jelínek, *Angew. Chem. Int. Ed.* **2022**, *61*, e202208010.
- [36] B. Lowe, J. Hellerstedt, A. Matěj, P. Mutombo, D. Kumar, M. Ondráček, P. Jelinek, A. Schiffrin, *J. Am. Chem. Soc.* **2022**, *144*, 21389–21397.
- [37] X.-L. Zhou, X.-Y. Zhu, J. M. White, *Surf. Sci. Rep.* **1991**, *13*, 73–220.
- [38] C. D. Lindstrom, X.-Y. Zhu, *Chem. Rev.* **2006**, *106*, 4281–4300.
- [39] J. Kubicki, H. L. Luk, Y. Zhang, S. Vyas, H.-L. Peng, C. M. Hadad, M. S. Platz, *J. Am. Chem. Soc.* **2012**, *134*, 7036–7044.
- [40] W. K. Peters, D. E. Couch, B. Mignolet, X. Shi, Q. L. Nguyen, R. C. Fortenberry, H. B. Schlegel, F. Remacle, H. C. Kapteyn, M. M. Murnane, W. Li, *Proc. Natl. Acad. Sci. USA* **2017**, *114*, E11072–E11081.
- [41] H.-L. Peng, *Phys. Chem. Chem. Phys.* **2018**, *20*, 29091–29104.
- [42] G. Burdzinski, J. C. Hackett, J. Wang, T. L. Gustafson, C. M. Hadad, M. S. Platz, *J. Am. Chem. Soc.* **2006**, *128*, 13402–13411.
- [43] J. Ghosh, S. Banerjee, A. Bhattacharya, *Chem. Phys.* **2017**, *494*, 78–89.
- [44] S. E. Braslavsky, *Pure Appl. Chem.* **2007**, *79*, 293–465.
- [45] I. D. Lemir, J. E. Argüello, A. E. Lanterna, J. C. Scaiano, *Chem. Commun.* **2020**, *56*, 10239–10242.

Manuscript received: January 31, 2025

Accepted manuscript online: February 24, 2025

Version of record online: March 6, 2025